Structural Engineering and Mechanics, *Vol. 66, No. 1 (2018) 125-138*
DOI: https://doi.org/10.12989/sem.2018.66.1.125

A transfer matrix method for in-plane bending vibrations of tapered beams with axial force and multiple edge cracks

Jung Woo Lee[a] and Jung Youn Lee*

Department of Mechanical System Engineering, Kyonggi University, 154-42, Gwanggyosan-ro, Yeongtong-gu, Suwon-si, Gyeonggi-do, 16227, Republic of Korea

(Received July 4, 2017, Revised February 26, 2018, Accepted February 27, 2018)

Abstract. This paper proposes a transfer matrix method for the bending vibration of two types of tapered beams subjected to axial force, and it is applied to analyze tapered beams with an edge or multiple edge open cracks. One beam type is assumed to be reduced linearly in the cross-section height along the beam length. The other type is a tapered beam in which the cross-section height and width with the same taper ratio is linearly reduced simultaneously. Each crack is modeled as two sub-elements connected by a rotational spring, and the method can evaluate the effect of cracking on the desired number of eigenfrequencies using a minimum number of subdivisions. Among the power series available for the solutions, the roots of the differential equation are computed using the Frobenius method. The computed results confirm the accuracy of the method and are compared with previously reported results. The effectiveness of the proposed methods is demonstrated by examining specific examples, and the effects of cracking and axial loading are carefully examined by a comparison of the single and double tapered beam results.

Keywords: transfer matrix method; Frobenius method; crack; axial force; tapered beam

1. Introduction

Dynamic characteristics analysis of non-uniform beams such as stepped and tapered beams have be widely used in engineering designs, and various approaches have been examined to obtain more accurate results for such problems. However, these structures experience cracking damage by various causes such as aging, environmental loads and manufacturing defects. The effect of cracks on the natural frequencies of damaged structures has been investigated using various approaches (Donà *et al.* 2015, Kisa and Gurel 2007, Lee and Chung 2000, Nahvi and Jabbari 2005, Broda *et al.* 2016, Neves *et al.* 2016); specifically, cracks reduced the natural frequencies. Wauer (1990) and Dimagoronas (1996) surveyed the approaches capable of evaluating the effect of cracking in rotating and non-rotating beams.

For vibrating structures having an arbitrary number of cracks, a number of investigators expressed the local displacements in the crack region as a rotational spring (Cheng *et al.* 2011, Skrinar 2009) and modeled the system as two sub-elements connected by this spring. Caddemi and Morassi (2013), and Caddemi and Calio (2009) studied the effect of multiple cracks on the natural frequencies of Euler-Bernoulli beams using the generalized functions. Some studies evaluated the effect of the crack using rotational and translational springs (Loya *et al.* 2006). Cracks in actual structures affect the bending stiffness in both the in-plane and out-of-plane directions, and these stiffnesses are reduced (Mazanoglu and Sabuncu 2010, Behzad *et al.* 2013). Fernández-Sáez *et al.* (2016) dealt with the inverse problems to analyze the effect of cracking based on natural frequency data. Cracked and twisted beams with bending displacements are coupled in two principal planes by twisting, and the variations of the local stiffness in the in-plane and out-of-plane directions should be considered (Lee and Lee 2017a). However, because the vibration in two directions can be decoupled from each other, the effect of the crack in such systems can be independently evaluated for the in-plane and out-of-plane directions when there is a straight cross-section.

For a non-uniform beam (Zhang and Yan 2016, Zhou *et al.* 2016, Sarkar and Ganguli 2014, Vinod *et al.* 2007, Yuan *et al.* 2016, Rossit *et al.* 2017, Sun *et al.* 2016, Sarkar *et al.* 2016), such problems have been studied over the past century to generate more accurate results using various methods such as the dynamic stiffness method (Banerjee *et al.* 2006) and the transfer matrix method (Lee and Lee 2016). The use of shape functions for non-uniform beams has also simplified the computational process (Banerjee *et al.* 2006), and power series has also been used to accurately determine the roots of the differential equation (Hodges and Rutkowski 1981). Among the power series solutions, the Frobenius method is preferred to investigate the bending vibration characteristics of a beam with a linearly variable cross-section height along the length of the beam. Kundu and Ganguli (2017) discussed the reason of buckling and the natural frequencies of rotating non-uniform beam with variable tensile and compressive forces using the Galerkin method.

Chaudhari and Maiti (1999) predicted the size and location of a crack for the bending vibration of a tapered

*Corresponding author, Professor
E-mail: jylee@kyonggi.ac.kr
[a]Ph.D.

ISSN: 1225-4568 (Print), 1598-6217 (Online)

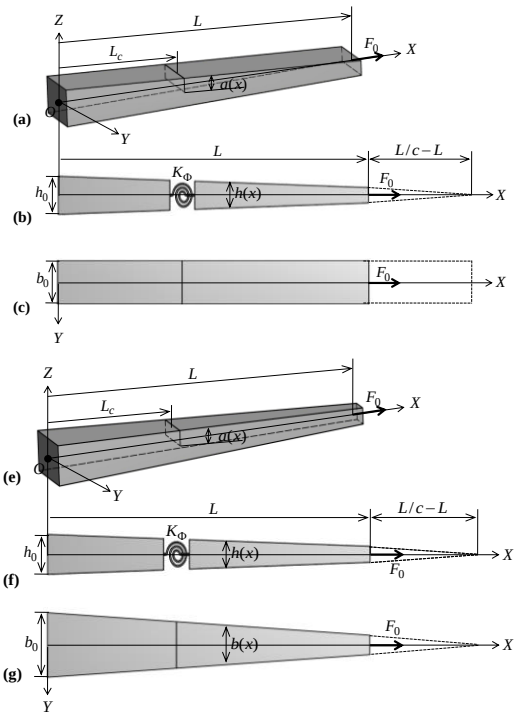

Fig. 1 Geometry of single and double tapered beams with an edge crack: (a) single tapered beam, (e) double tapered beam, (b,f) side view, and (c,g) top view

beam with a linearly reduced cross-section height using the Frobenius method. Using the roots of the differential equation computed from the Frobenius method, Lee and Lee (2017b) used the transfer matrix approach to investigate the effect of cracking on the natural frequencies of rotating straight beams. However, this method does not consider the effect of tapering. Additionally, the present method uses the transfer matrix method to determine the natural frequencies of a tapered beam with axial loading and multiple open edge cracks. The transfer matrix method has an advantage that the effect of a crack can be simply multiplied in the transfer of the state quantities because the global matrix is the same regardless of the number of subdivisions (Lee and Lee 2017a, b, Attar 2012). In addition, there is a dearth of studies on tapered beams with axial force and cracking, though the effect of cracks on the natural frequencies for bending vibrations of single or double tapered beams has been reported (Mazanoglu and Sabuncu 2010, Chaudhari and Maiti 1999). However, the present authors could not locate investigations in which a direct comparison is made between the results obtained from two types of tapered beams.

The objective of this study is to propose a simple numerical method capable of providing more accurate results for the in-plane bending vibrations of two types of axially loaded and tapered beams with an edge or multiple edge open cracks at arbitrary locations and then to use this method to analyze the effect on the natural frequencies in the beam structures. The present method has the advantage that it can produce the desired number of accurate results using a minimum number of sub-elements. The local displacements of the crack region in this study are modeled

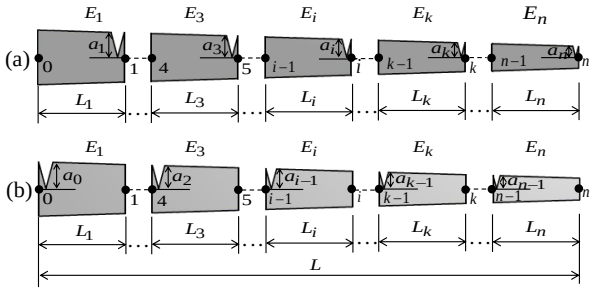

Fig. 2 The subdivided elements of a beam with an edge crack for the transfer matrix method; (a) the beam element with multiple cracks at the right-hand end, and (b) the beam element with multiple cracks at the left-hand end

as two segments connected by a rotational spring, and the additional displacement generated by the bending moment caused by the crack is formulated as an independent transfer matrix (Lee and Lee 2017a, b). To demonstrate the accuracy of the method, the computed results are compared with the natural frequencies discussed in previous works. The effect of cracking in tapered beams is also examined through a parametric study with respect to various sizes and locations of crack, and a comprehensive analysis between single and double tapered beams is presented.

2. Theory

This study did not consider the effect of rotary inertia and shear deformation. Instead, it investigates the in-plane bending vibration of axially loaded single and double tapered beams with multiple edge open cracks. Additionally, longitudinal vibration is ignored and open cracks are assumed. When the beam element has a single edge crack, two types of axially loaded tapered beams with a crack are illustrated in Fig. 1, where XYZ are the global coordinates, L is the length of the beam element, c is the taper ratio, K_Φ is the rotational spring, and a is the size of cracking. h_0 and b_0 are the height and width of a cross-section when $c = 0$, respectively. $h(x)$ and $b(x)$ are the height and width of a cross-section at arbitrary locations, respectively, in which the dimension of the cross-section is reduced by a taper ratio c. $a(x)$ is the variation of the size of the crack by the taper ratio, and F_0 is the constant axial force.

In Fig. 1, $a(x)$, $h(x)$, and $b(x)$ can be expressed by

$$a(x) = a_0\left(1 - c\frac{x}{L}\right),$$
$$h(x) = h_0\left(1 - c\frac{x}{L}\right),\ b(x) = b_0\left(1 - c\frac{x}{L}\right) \tag{1}$$

From Eq. (1), the ratio of the crack depth (s) with respect to the height of the beam cross-section is given as

$$s = \frac{a(x)}{h(x)} = \frac{a_0(1-\zeta)}{h_0(1-\zeta)} = \frac{a_0}{h_0} \tag{2}$$

where the non-dimensional length parameter of the beam element can be introduced as $\bar{x}(= 1 - \zeta)$ and $\zeta = c\,x/L$.

In addition, ζ can be expressed as $1-\bar{x}$, and x/L is used for $\bar{L}$ for convenience.

To use the transfer matrix method for two types of tapered beams with multiple edge cracks, the segments are illustrated in Fig. 2. Fig. 2(a) is the element model with cracks at the right-hand end of the element, and Fig. 2(b) is the cracked beam model at the left-hand end of the element. The present method can produce the desired number of eigenfrequencies using two subdivisions when the beam-like structures have a crack, and the number of these elements is varied as a function of the number of cracks.

2.1 Local displacement of the crack region

As illustrated in Fig. 1, two types of axially loaded and tapered beams with an edge crack were modeled as two sub-elements connected by a rotational spring for the in-plane bending vibration. An expression for the local displacement of the cracked region was selected from previous literature (Chondros *et al.* 1998). The additional displacement (Φ^*) generated by the crack can be expressed as

$$\Phi^* = \frac{6\pi(1-\upsilon^2)Mh(x)f(s)}{EI(x)} \tag{3}$$

where

$$\begin{aligned} f(s) = {} & 0.6272s^2 - 1.04533s^3 + 4.5948s^4 \\ & -9.9736s^5 + 20.2948s^6 - 33.035s^7 \\ & +47.1063s^8 - 40.7556s^9 + 19.6s^{10} \end{aligned} \tag{4}$$

and υ is Poisson's ratio. $EI(x)$ and $I(x)$ are the variations of the bending stiffness and the moment of inertia over the beam cross-section according to the taper ratio, respectively, and E and M are the elastic modulus of the beam and bending moment, respectively.

The variation of the bending stiffness for a tapered beam can be expressed as

$$EI(x) = EI_0(1-\zeta)^{n+2} \tag{5}$$

where EI_0 is the bending stiffness for c=0, and n=1 for a single tapered beam and n=2 for a double tapered beam.

Substituting Eqs. (1) and (5) into Eq. (3), Φ^* can be rewritten as

$$\begin{aligned} \Phi^* &= \frac{6\pi(1-\upsilon^2)Mh_0(1-\zeta)f(s)}{EI_0(1-\zeta)^{n+2}} \\ &= \frac{6\pi(1-\upsilon^2)Mh_0f(s)}{EI_0(1-\zeta)^{n+1}} \end{aligned} \tag{6}$$

The rotational spring stiffness of the cracked region from Eq. (6) can be deduced by

$$K_\Phi = \frac{EI_0(1-\zeta)^{n+1}}{6\pi(1-\upsilon^2)h_0f(s)} \tag{7}$$

2.2 Element transfer matrix of tapered beams with axial force

The differential equation, the bending moment, and the shear deformation for axially loaded and tapered beams with a linearly reduced cross-section can be derived as (Banerjee *et al.* 2006)

$$\big(EI(x)w''(x,t)\big)'' - F_0w''(x,t) + m(x)\ddot{w}(x,t) = 0 \tag{8}$$

$$M(x,t) = -EI(x)w''(x,t) \tag{9}$$

$$V(x,t) = \big(EI(x)w''(x,t)\big)' - F_0w'(x,t) \tag{10}$$

where $M(x,t)$ denote the bending moment, $V(x,t)$ indicate the shear force and $w(x,t)$ is the in-plane bending displacement. The prime and the dots indicate differentiation with respect to the distance x and time t, respectively.

The mass variation along the length of the structures by the taper ratio can be expressed as

$$m(x) = m_0(1-\zeta)^n \tag{11}$$

where m_0 is the mass per unit length for c=0.

When the general solution of Eq. (8) assumes harmonic vibrations with an angular frequency (ω)

$$w(x,t) = W(x)\cos\omega t \tag{12}$$

where $W(x)$ is the amplitude of $w(x,t)$.

When substituting Eq. (12) into Eq. (8), the variables with respect to time and distance can be integrated into a variable of distance x as

$$\begin{aligned} EI(x)W'''' + 2EI'(x)W''' + EI''(x)W'' - F_0W'' \\ -m(x)\omega^2W = 0 \end{aligned} \tag{13}$$

where $W = W(x)$

2.2.1 Single tapered beam (when n=1)

A tapered beam with a linearly reduced cross-section height occurs when substituting n=1 into Eqs. (5) and (11). Thus, if these equations are substituted into Eq. (13), the differential equation in non-dimensional form is given by

$$\begin{aligned} (\zeta^3 - 3\zeta^2 + 3\zeta - 1)W'''' + 6(\zeta^2 - 2\zeta + 1)W''' \\ +(6\zeta - C_1)W'' + C_2(\zeta - 1)W = 0 \end{aligned} \tag{14}$$

where

$$C_1 = 6 - C_3, C_2 = -\frac{m_0\omega^2L^4}{EI_0c^4}, C_3 = \frac{F_0L^2}{EI_0c^2} \tag{15}$$

The roots of Eq. (14) can be computed using the Frobenius method, and the general solution is expressed by

$$W(\zeta,k) = \sum_{i=0}^{\infty} a_{i+1}(k)\,\zeta^{k+i} \tag{16}$$

By substituting the appropriate differentiation forms of Eq. (16) into Eq. (14), the indicial equation is obtained by

$$k(k-1)(k-2)(k-3)a_1 = 0 \tag{17}$$

The equation for the recurrence relationship that can determine the general coefficients, is obtained by

$$\begin{aligned} a_{i+5} = {} & \frac{3(k+i+2)}{(k+i+4)}a_{i+4} \\ & -\frac{3(k+i)(k+i-1)+12(k+i)+C_1}{(k+i+4)(k+i+3)}a_{i+3} \\ & +\frac{(k+i)\{(k+i-1)(k+i-2)+6(k+i-1)+6\}}{(k+i+4)(k+i+3)(k+i+2)}a_{i+2} \\ & -\frac{C_2}{(k+i+4)(k+i+3)(k+i+2)(k+i+1)}a_{i+1} \\ & +\frac{C_2}{(k+i+4)(k+i+3)(k+i+2)(k+i+1)}a_i \end{aligned} \tag{18}$$

From Eqs. (17) and (18), the Frobenius coefficients $a_1 - a_5$ can be produced as

$$\begin{gathered} a_1 = 1, \quad a_2 = \frac{3(k-1)}{(k+1)} a_1 \\ a_3 = \frac{3k}{(k+2)} a_2 - \frac{3(k-2)(k+1)+C_1}{(k+2)(k+1)} a_1 \\ a_4 = \frac{3(k+1)}{(k+3)} a_3 - \frac{3(k-1)(k-2)+12(k-1)+C_1}{(k+3)(k+2)} a_2 \\ + \frac{(k-1)(k-2)(k-3)+6(k-1)(k-2)+6(k-1)}{(k+3)(k+2)(k+1)} a_1 \\ a_5 = \frac{3(k+2)}{(k+4)} a_4 - \frac{3k(k-1)+12k+C_1}{(k+4)(k+3)} a_3 \\ + \frac{k(k-1)(k-2)+6k(k-1)+6k}{(k+4)(k+3)(k+2)} a_2 \\ - \frac{C_2}{(k+4)(k+3)(k+2)(k+1)} a_1 \end{gathered} \tag{19}$$

In addition, the solution of the differential equation by multiplying four arbitrary constants for four values of the index k can be expressed as

$$\begin{aligned} W(\zeta) = A_1 f(\zeta, 0) + A_2 f(\zeta, 1) + A_3 f(\zeta, 2) \\ + A_4 f(\zeta, 3) \end{aligned} \tag{20}$$

where A_1, A_2, A_3 and A_4 are arbitrary constants, and $f(\zeta, k)$ for the four roots of the indicial equation is given by

$$f(\zeta, k) = \sum_{i=0}^{\infty} a_{i+1}(k)\, \zeta^{k+i} \tag{21}$$

The slope of the deformation curve (Φ) can be obtained by differentiating Eq. (20)

$$\begin{aligned} \Phi = \frac{c}{L}\frac{dW(\zeta)}{d\zeta} = \frac{c}{L}\{A_1 f'(\zeta, 0) + A_2 f'(\zeta, 1) \\ + A_3 f'(\zeta, 2) + A_4 f'(\zeta, 3)\} \end{aligned} \tag{22}$$

By substituting Eqs. (5) and (11) into Eqs. (9) and (10), the expression of the bending moment and shear force can be rewritten by

$$M = N_1 (1-\zeta)^3 \frac{d^2 W(\zeta)}{d\zeta^2} \tag{23}$$

$$\begin{aligned} V = N_2 \left((1-\zeta)^3 \frac{d^3 W(\zeta)}{d\zeta^3} - 3(1-\zeta)^2 \frac{d^2 W(\zeta)}{d\zeta^2} \right. \\ \left. - C_3 \frac{dW(\zeta)}{d\zeta} \right) \end{aligned} \tag{24}$$

where

$$N_1 = -\frac{EI_0 c^2}{L^2}, N_2 = \frac{EI_0 c^3}{L^3} \tag{25}$$

2.2.2 Double tapered beam (when n=2)

A tapered beam with linearly reduced cross-section height and width at the same taper ratio occurs when substituting n=2 into Eqs. (5) and (11). Thus, if these equations are substituted into Eq. (13), the differential equation in non-dimensional form is given by

$$\begin{aligned} (\zeta^4 - 4\zeta^3 + 6\zeta^2 - 4\zeta + 1) W'''' \\ + 8(\zeta^3 - 3\zeta^2 + 3\zeta - 1) W''' \\ + (12\zeta^2 - 24\zeta + D_1) W'' \\ + D_2(\zeta^2 - 2\zeta + 1) W = 0 \end{aligned} \tag{26}$$

where

$$D_1 = 12 - D_3, D_2 = -\frac{m_0 \omega^2 L^4}{EI_0 c^4}, D_3 = \frac{F_0 L^2}{EI_0 c^2} \tag{27}$$

By substituting the appropriate differentiation forms of Eq. (16) into Eq. (26), the following equation is obtained

$$\begin{aligned} a_{i+6} = \frac{4(k+i+3)}{(k+i+5)} a_{i+5} \\ - \frac{6(k+i+4)(k+i+1)+D_1}{(k+i+5)(k+i+4)} a_{i+4} \\ + \frac{\{4(k+i+5)(k+i)+24\}(k+i+1)}{(k+i+5)(k+i+3)(k+i+4)} a_{i+3} \\ - \frac{\{(k+i+6)(k+i-1)+12\}(k+i+1)(k+i)+D_2}{(k+i+5)(k+i+2)(k+i+3)(k+i+4)} \\ + \frac{2D_2}{(k+i+5)(k+i+2)(k+i+3)(k+i+4)} a_{i+1} \\ - \frac{D_2}{(k+i+5)(k+i+2)(k+i+3)(k+i+4)} a_i \end{aligned} \tag{28}$$

Eq. (28) is the equation for the recurrence relationship that can determine the general coefficients, and the indicial equations for single and double tapered beams are identical.

From Eqs. (17) and (28), the Frobenius coefficients $a_1 - a_6$ can be produced as

$$\begin{gathered} a_1 = 1, \quad a_2 = \frac{4(k-1)}{(k+1)} a_1 \\ a_3 = \frac{4k}{(k+2)} a_2 - \frac{6(k+1)(k-2)+D_1}{(k+2)(k+1)} a_1 \\ a_4 = \frac{4(k+1)}{(k+3)} a_3 - \frac{6(k+2)(k-1)+D_1}{(k+3)(k+2)} a_2 \\ + \frac{\{4(k+3)(k-2)+24\}(k-1)}{(k+3)(k+1)(k+2)} a_1 \\ a_5 = \frac{4(k+2)}{(k+4)} a_4 - \frac{6(k+3)k+D_1}{(k+4)(k+3)} a_3 \\ + \frac{\{4(k+4)(k-1)+24\}k}{(k+4)(k+2)(k+3)} a_2 \\ - \frac{\{(k+5)(k-2)+12\}k(k-1)+D_2}{(k+1)(k+2)(k+3)(k+4)} a_1 \\ a_6 = \frac{4(k+3)}{(k+5)} a_5 - \frac{6(k+4)(k+1)+D_1}{(k+5)(k+4)} a_4 \\ + \frac{\{4k(k+5)+24\}(k+1)}{(k+i+5)(k+i+3)(k+i+4)} a_3 \\ - \frac{k(k+1)\{(k+6)(k-1)+12\}+D_2}{(k+5)(k+2)(k+3)(k+4)} a_2 \\ + \frac{2D_2}{(k+2)(k+3)(k+4)(k+5)} a_1 \end{gathered} \tag{29}$$

By substituting Eqs. (5) and (11) into Eqs. (9) and (10), the expression of the bending moment and shear force can be rewritten by

$$M = N_1 (1-\zeta)^4 \frac{d^2 W(\zeta)}{d\zeta^2} \tag{30}$$

and

$$\begin{aligned} V = N_2 \left((1-\zeta)^4 \frac{d^3 W(\zeta)}{d\zeta^3} - 4(1-\zeta)^3 \frac{d^2 W(\zeta)}{d\zeta^2} \right. \\ \left. - D_3 \frac{dW(\zeta)}{d\zeta} \right) \end{aligned} \tag{31}$$

Similarly, the expression for Eqs. (20) and (22) can be used for n=2.

Consider a k-th element without cracks between points $k-1$ and k in Fig. 2(a). The element transfer matrix of the k-th element can be obtained by substituting any valid values in place of the distance x into Eqs. (20), (22), (23), (24), (30), and (31). The length x of the beam element is zero at point $k-1$ and is L_k at point k. Therefore, if $x=0$ is substituted into Eqs. (20), (22), (23), (24), (30), and (31), these equations are given by

For n=1

$$W_{k-1}=\sum_{j=1}^{4}A_j f(0,j-1) \tag{32}$$

$$\Phi_{k-1}=\frac{c}{L}\sum_{j=1}^{4}A_j f'(0,j-1) \tag{33}$$

$$M_{k-1}=N_1\sum_{j=1}^{4}A_j f''(0,j-1) \tag{34}$$

$$\begin{aligned}V_{k-1}=N_2\Bigg(&\sum_{j=1}^{4}A_j f'''(0,j-1)\\&-3\sum_{j=1}^{4}A_j f''(0,j-1)\\&-C_3\sum_{j=1}^{4}A_j f'(0,j-1)\Bigg)\end{aligned} \tag{35}$$

For n=2

$$M_{k-1}=N_1(1-\zeta)^4\sum_{j=1}^{4}A_j f''(0,j-1) \tag{36}$$

$$\begin{aligned}V_{k-1}=N_2\Bigg(&\sum_{j=1}^{4}A_j f'''(0,j-1)\\&-4\sum_{j=1}^{4}A_j f''(0,j-1)\\&-D_3\sum_{j=1}^{4}A_j f'(0,j-1)\Bigg)\end{aligned} \tag{37}$$

When expressing Eqs. (32)-(37) in matrix form, the state quantities at point $k-1$ can be determined to be

$$\begin{Bmatrix}W_{k-1}\\ \Phi_{k-1}\\ M_{k-1}\\ V_{k-1}\end{Bmatrix}=\begin{bmatrix}H_{11}&H_{12}&H_{13}&H_{14}\\ H_{21}&H_{22}&H_{23}&H_{24}\\ H_{31}&H_{32}&H_{33}&H_{34}\\ H_{41}&H_{42}&H_{43}&H_{44}\end{bmatrix}\begin{Bmatrix}A_1\\ A_2\\ A_3\\ A_4\end{Bmatrix} \tag{38}$$

Eq. (38) can be simplified as

$$\mathbf{Z}_{k-1}=\mathbf{H}\mathbf{A} \tag{39}$$

The arbitrary constants $\mathbf{A}$ can be determined from Eq. (39), and it is clear that

$$\mathbf{A}=\mathbf{H}^{-1}\mathbf{Z}_{k-1} \tag{40}$$

In a similar way, substituting $x=L_k$ into Eqs. (20), (22), (23), (24), (30), and (31) yields

For n=1

$$W_k=\sum_{j=1}^{4}A_j f(c,j-1) \tag{41}$$

$$\Phi_k=\frac{c}{L}\sum_{j=1}^{4}A_j f'(c,j-1) \tag{42}$$

$$M_k=N_1(1-c)^3\sum_{j=1}^{4}A_j f''(c,j-1) \tag{43}$$

$$\begin{aligned}V_k=N_2\Bigg((1-c)^3&\sum_{j=1}^{4}A_j f'''(c,j-1)\\&-3(1-c)^2\sum_{j=1}^{4}A_j f''(c,j-1)\\&-C_3\sum_{j=1}^{4}A_j f'(c,j-1)\Bigg)\end{aligned} \tag{44}$$

For n=2

$$M_k=N_1(1-c)^4\sum_{j=1}^{4}A_j f''(c,j-1) \tag{45}$$

$$\begin{aligned}V_k=N_2\Bigg((1-c)^4&\sum_{j=1}^{4}A_j f'''(c,j-1)\\&-4(1-c)^3\sum_{j=1}^{4}A_j f''(c,j-1)\\&-D_3\sum_{j=1}^{4}A_j f'(c,j-1)\Bigg)\end{aligned} \tag{46}$$

From Eqs. (41)-(46), the state quantities at point k can be obtained by

$$\begin{Bmatrix}W_k\\ \Phi_k\\ M_k\\ V_k\end{Bmatrix}=\begin{bmatrix}Q_{11}&Q_{12}&Q_{13}&Q_{14}\\ Q_{21}&Q_{22}&Q_{23}&Q_{24}\\ Q_{31}&Q_{32}&Q_{33}&Q_{34}\\ Q_{41}&Q_{42}&Q_{43}&Q_{44}\end{bmatrix}\begin{Bmatrix}A_1\\ A_2\\ A_3\\ A_4\end{Bmatrix} \tag{47}$$

Eq. (47) can be simplified as

$$\mathbf{Z}_k=\mathbf{Q}\mathbf{A} \tag{48}$$

Table 1 Comparison of the first three natural frequencies computed between the present method and previous work for a uniform beam with two edge cracks

Approaches			Natural frequency (rad/s)		
			1	2	3
Experimental measurements (Ruotolo and Surace 1997)		Intact beam	151.896	955.691	2666.93
		Cracked beam	151.073	937.878	2571.63
Lee and Lee (2017a, b), Attar (2012)		Intact beam	152.208	953.873	2670.87
Lee and Lee (2017a, b)		Cracked beam	151.140	938.398	2588.87
Attar (2012)		Cracked beam	151.058	937.405	2583.64
Lee (2009)	Rotational spring (k=k_1)	Cracked beam	151.456	939.588	2588.92
	Rotational spring (k=k_2)	Cracked beam	151.708	943.232	2607.65
Yan *et al.* (2016)	Model No. 3	Cracked beam	151.135	938.39	2588.9
Present	n=1	Intact beam	152.170	953.401	2669.27
		Cracked beam	151.103	937.968	2587.52
	n=2	Intact beam	152.200	953.494	2669.43
		Cracked beam	151.134	938.072	2587.73

Table 2 Comparison of the first three natural frequencies for an axially loaded uniform beam with a C-F end condition

ω			Non-dimensional natural frequency					
			Axial loading					
			–5	–3	0	4	7	15
1	Li *et al.* (2013)		-	-	3.51602	5.42082	6.38302	8.24969
	Present	n=1	-	-	3.51641	5.42246	6.38505	8.25236
		n=2	-	-	3.51749	5.42444	6.38740	8.25536
2	Li *et al.* (2013)		17.96309	19.69280	22.03449	24.77594	26.60999	30.83900
	Present	n=1	17.95043	19.68279	22.02762	24.77209	26.60782	30.83990
		n=2	17.94966	19.68330	22.02970	24.77577	26.61244	30.84639
3	Li *et al.* (2013)		58.48225	59.78843	61.69721	64.15264	65.93092	70.43175
	Present	n=1	58.45111	59.75907	61.67036	64.12883	65.90918	70.41484
		n=2	58.45097	59.75981	61.67235	64.13238	65.91381	70.42202

By substituting Eq. (40) into Eq. (48), the relationship between the state vectors $\mathbf{Z}_k$ and $\mathbf{Z}_{k-1}$ can be expressed by

$$\mathbf{Z}_k = \mathbf{T}_k \mathbf{Z}_{k-1} \tag{49}$$

where $\mathbf{T}_k = \mathbf{Q}\mathbf{H}^{-1}$ is the element transfer matrix of the k-th element.

2.3 Transfer matrix of tapered beams with single or multiple edge cracks

When considering an element between points $k-1$ and k, as shown in Fig. 2(a), the additional displacement generated by cracking with the help of Eq. (7) is expressed in the form of a matrix as

$$\begin{Bmatrix} W_k \\ \Phi_k \\ M_k \\ V_k \end{Bmatrix} = \begin{bmatrix} 1 & 0 & 0 & 0 \\ 0 & 1 & -K_\phi^* & 0 \\ 0 & 0 & 1 & 0 \\ 0 & 0 & 0 & 1 \end{bmatrix}_k \begin{Bmatrix} W_{k-1} \\ \Phi_{k-1} \\ M_{k-1} \\ V_{k-1} \end{Bmatrix} \tag{50}$$

where K_ϕ^* is equal to $1/K_\Phi$.

Eq. (50) can be simplified as

$$\mathbf{Z}_k = \mathbf{K}_k \mathbf{Z}_{k-1} \tag{51}$$

As shown in Fig. 2(a) and 2(b), the element transfer matrix of tapered beams with multiple cracks at arbitrary locations can be assembled as follows

$$\mathbf{T} = \mathbf{T}_n \times \cdots \times \mathbf{K}_k \times \mathbf{T}_k \times \mathbf{K}_j \times \mathbf{T}_j \times \cdots \times \mathbf{K}_1 \times \mathbf{T}_1 \tag{52}$$

or

$$\mathbf{T} = \mathbf{T}_n \times \mathbf{K}_{n-1} \times \cdots \times \mathbf{T}_k \times \mathbf{K}_{k-1} \times \cdots \times \mathbf{T}_1 \times \mathbf{K}_0 \tag{53}$$

Eq. (52) can be evaluated using the Fig. 2(a) model, and Eq. (53) can be evaluated using the Fig. 2(b) model for two types of tapered beams with an edge crack.

Therefore, the state vectors $\mathbf{Z}_0$ and $\mathbf{Z}_L$ on the left- and right-hand sides of the total length of the tapered beams have the following relationship

$$\mathbf{Z}_L = \mathbf{T}\mathbf{Z}_0 \tag{54}$$

The global transfer matrix of Eq. (54) can be used to analyze the natural frequencies of axially loaded tapered

Table 3 The results computed from two types of tapered beams having the axial loading at the free end when c=0 and 0.5

		Natural frequency (Hz)										
	ω	Tensile loading (F_0)						Compressive loading (F_0)				
		0N	100N	200N	300N	400N	500N	–100N	–200N	–300N	–400N	–500N
n=1	1	12.742	13.044	13.337	13.622	13.900	14.171	12.430	12.108	11.775	11.429	11.070
c=0	2	79.817	80.158	80.497	80.835	81.171	81.505	79.475	79.131	78.785	78.437	78.088
	3	223.46	223.75	224.04	224.33	224.62	224.91	223.17	222.88	222.59	222.30	222.00
	4	437.88	438.16	438.43	438.71	438.98	439.25	437.61	437.34	437.06	436.79	436.51
n=1	1	13.855	14.401	14.914	15.399	15.860	16.299	13.273	12.647	11.969	11.228	10.409
c=0.5	2	66.373	67.148	67.910	68.659	69.396	70.121	65.584	64.782	63.965	63.133	62.285
	3	171.26	171.97	172.68	173.38	174.07	174.77	170.55	169.84	169.12	168.39	167.66
	4	327.75	328.41	329.08	329.74	330.40	331.05	327.08	326.41	325.75	325.07	324.40
n=2	1	12.746	13.048	13.342	13.627	13.905	14.175	12.434	12.112	11.778	11.433	11.073
c=0	2	79.825	80.166	80.505	80.843	81.179	81.514	79.482	79.138	78.792	78.444	78.095
	3	223.47	223.76	224.05	224.34	224.63	224.92	223.18	222.89	222.60	222.30	222.01
	4	437.89	438.17	438.44	438.72	438.99	439.26	437.62	437.34	437.07	436.79	436.52
n=2	1	16.759	17.554	18.285	18.963	19.595	20.189	15.887	14.919	13.828	12.572	11.086
c=0.5	2	70.831	72.040	73.215	74.357	75.468	76.551	69.586	68.303	66.980	65.616	64.207
	3	176.03	177.18	178.31	179.44	180.55	181.66	174.86	173.69	172.51	171.31	170.10
	4	332.68	333.77	334.85	335.92	336.99	338.05	331.59	330.50	329.40	328.29	327.18

Table 4 Effect of axial loading on the first four natural frequencies of tapered beams with a C-F end condition as a function of location when c=0.5

	ω	Natural frequency (Hz)									
		$\bar{L}$=0.1	$\bar{L}$=0.2	$\bar{L}$=0.3	$\bar{L}$=0.4	$\bar{L}$=0.5	$\bar{L}$=0.6	$\bar{L}$=0.7	$\bar{L}$=0.8	$\bar{L}$=0.9	$\bar{L}$=1
n=1	1	13.860	13.889	13.968	14.114	14.343	14.657	15.046	15.480	15.914	16.299
F_0=500N	2	66.391	66.483	66.628	66.744	66.776	66.799	67.031	67.706	68.839	70.121
	3	171.30	171.43	171.49	171.51	171.73	172.14	172.32	172.41	173.22	174.77
	4	327.81	327.90	327.92	328.17	328.41	328.46	328.88	329.14	329.48	331.05
n=2	1	16.764	16.799	16.897	17.087	17.396	17.838	18.402	19.042	19.671	20.189
F_0=500N	2	70.851	70.956	71.132	71.282	71.327	71.358	71.696	72.739	74.552	76.551
	3	176.07	176.20	176.28	176.31	176.59	177.15	177.41	177.55	178.97	181.66
	4	332.74	332.85	332.87	333.17	333.49	333.55	334.18	334.57	335.19	338.05
n=1	1	13.851	13.821	13.740	13.585	13.338	12.990	12.536	11.974	11.286	10.409
F_0= –500N	2	66.354	66.261	66.114	65.999	65.967	65.942	65.699	65.004	63.815	62.285
	3	171.23	171.10	171.04	171.02	170.79	170.38	170.20	170.11	169.28	167.66
	4	327.69	327.60	327.58	327.33	327.08	327.03	326.61	326.35	326.00	324.40
n=2	1	16.754	16.719	16.617	16.415	16.078	15.581	14.904	14.018	12.841	11.086
F_0= –500N	2	70.811	70.705	70.527	70.377	70.333	70.299	69.940	68.855	66.904	64.207
	3	175.98	175.85	175.77	175.74	175.45	174.89	174.63	174.48	173.04	170.10
	4	332.62	332.52	332.49	332.19	331.88	331.81	331.18	330.79	330.15	327.18

beams with single or multiple edge cracks using different boundary conditions (Lee and Lee 2017b).

3. Results and discussion

To validate the accuracy of the proposed two methods, the predicted natural frequencies are compared with the results presented in previous works (Lee and Lee 2017a, b, Attar 2012, Lee 2009, Li *et al.* 2013, Ruotolo and Surace 1997, Yan *et al.* 2016). In the present transfer matrix methods, because the taper ratio (c) does not allow zero to be set exactly for the computation of the homogeneous solutions for the uniform beams, the valid value used is c=0.001. The compared properties include: $E = 181GPa$, $\rho = 7860kg/m^3$, $L = 0.8m$, $h = 0.02m$, $b = 0.02m$,

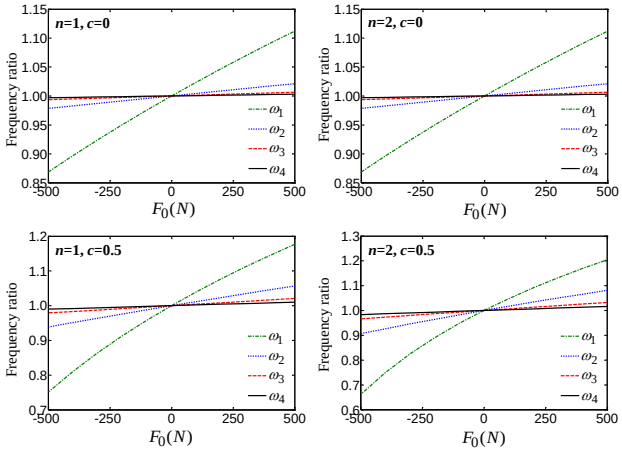

Fig. 3 Effect of axial loading on the first four natural frequencies of tapered beams when c=0 and 0.5

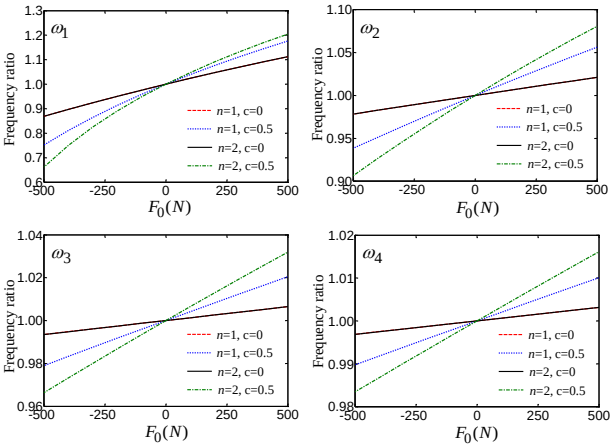

Fig. 4 Comparison of each mode computed between n=1 and n=2 when c=0 and c=0.5

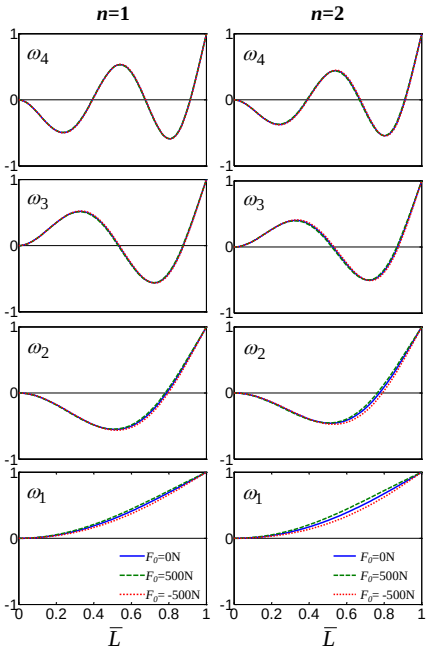

Fig. 5 Effect of axial loading on the first four mode shapes of tapered beams when c=0.5

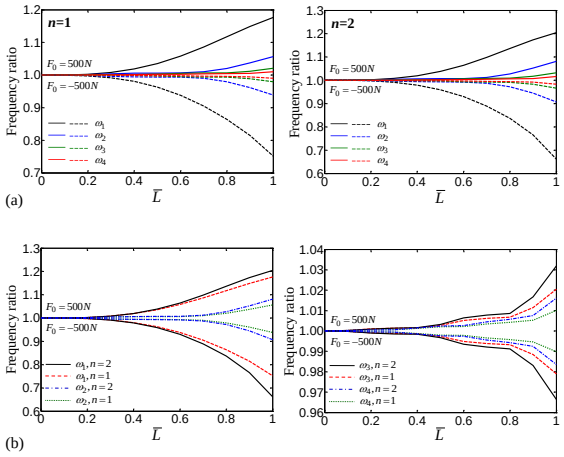

Fig. 6 Comparison of the tensile and compressive loadings for tapered beams

$\nu = 0.29$.

Double edge open cracks are assumed to exist at cracks of s=0.2 and 0.3 at distances 0.25456 m and 0.54496 m, respectively, from the fixed end when the beam element adopts a clamped-free end condition. A comparison of the literature results of those derived from the proposed method are given in Table 1. As seen, excellent agreement of the natural frequencies is obtained. The present methods are proposed to analyze the natural frequencies for the in-plane bending vibration of tapered beams with multiple cracks and axial loading. However, the approaches can also be used to calculate the homogeneous solutions for uniform beams with sufficient accuracy, as shown in Table 1. The Lee and Lee (2017b) results are those computed for the present example using the transfer matrix method to compare with their previous work Lee and Lee (2017a).

In this regard, the effect of axial loading on the first three non-dimensional natural frequencies of a uniform beam is compared between the results computed from the present methods and those given in the previous work. The results are listed in Table 2, which shows excellent agreement.

3.1 The effect of axial loading

Based on the results presented above, the effect of compressive and tensile loadings on the first four natural frequencies of uniform, single (n=1) and double (n=2) tapered beams have been investigated (Tables 3 and 4). The axial loading (F_0) has been increased from -500 N to 500N in intervals of 100N, and the considered taper ratios are c=0 and c=0.5. The properties of the examined beam are: $E = 200GPa$, $\rho = 7850kg/m^3$, $L = 0.8m$, $h = 0.01m$, $b = 0.03m$, $\nu = 0.3$.

When n=1 and n=2, the effect of axial loading on the first four eigenfrequencies for each case can be easily seen in Figs. 3 and 4. Fig. 3 presents the frequency ratio with respect to axial loading, and Fig. 4 compares the results computed from n=1 and n=2 for each mode. As seen, the effects on the natural frequencies are larger for the fundamental frequency, and the effect of axial loading

Table 5 Effect of cracking on the first four eigenfrequencies of a single tapered beam with different end conditions with respect to the variation of the crack's locations given c=0.5, s=0.5 and F_0=0

BCs	ω	Intact	Natural frequency (Hz)								
			$\bar{L}_c$=0.1	$\bar{L}_c$=0.2	$\bar{L}_c$=0.3	$\bar{L}_c$=0.4	$\bar{L}_c$=0.5	$\bar{L}_c$=0.6	$\bar{L}_c$=0.7	$\bar{L}_c$=0.8	$\bar{L}_c$=0.9
C-F	1	13.855	13.253	13.379	13.501	13.612	13.707	13.779	13.825	13.848	13.855
	2	66.373	64.854	66.120	66.316	65.633	64.809	64.543	65.026	65.837	66.313
	3	171.26	169.89	170.79	167.64	167.57	170.61	170.53	167.16	167.15	170.47
	4	327.75	327.48	321.85	321.38	327.75	321.21	321.96	327.47	319.59	323.83
C-C	1	59.192	57.579	58.795	59.191	58.838	58.254	58.044	58.457	59.099	58.905
	2	162.99	161.53	162.63	159.61	159.10	161.94	162.71	160.15	160.38	162.99
	3	319.37	319.05	313.78	312.82	319.33	313.37	312.89	319.35	313.44	318.24
	4	527.82	527.45	514.65	527.03	516.51	522.13	522.07	518.74	524.74	521.93
C-P	1	44.570	43.200	44.073	44.526	44.499	44.140	43.749	43.607	43.838	44.299
	2	135.98	134.39	135.91	133.88	132.52	134.05	135.93	134.86	132.93	134.02
	3	279.45	278.88	275.60	272.82	278.64	276.66	272.28	278.31	276.80	273.64
	4	474.95	474.86	463.20	472.72	467.96	465.80	473.85	463.45	474.95	464.61
S-S	1	25.805	25.762	25.633	25.447	25.258	25.130	25.111	25.223	25.443	25.685
	2	104.91	104.08	102.39	101.72	102.80	104.49	104.75	103.33	102.45	103.62
	3	235.45	231.56	228.44	232.72	235.22	230.39	230.51	235.35	232.18	230.83
	4	417.98	407.78	409.98	417.68	407.18	414.58	413.86	409.05	417.65	408.70

Table 6 Effect of cracking on the first four eigenfrequencies of a double tapered beam with different end conditions with respect to the variation of the crack's locations given c=0.5, s=0.5 and F_0=0

BCs	ω	Intact	Natural frequency (Hz)								
			$\bar{L}_c$=0.1	$\bar{L}_c$=0.2	$\bar{L}_c$=0.3	$\bar{L}_c$=0.4	$\bar{L}_c$=0.5	$\bar{L}_c$=0.6	$\bar{L}_c$=0.7	$\bar{L}_c$=0.8	$\bar{L}_c$=0.9
C-F	1	16.759	16.062	16.189	16.321	16.449	16.564	16.655	16.717	16.748	16.758
	2	70.831	69.118	70.484	70.802	70.142	69.238	68.885	69.357	70.231	70.763
	3	176.03	174.44	175.65	172.41	172.08	175.22	175.39	171.93	171.79	175.19
	4	332.68	332.31	326.93	325.95	332.66	326.28	326.66	332.45	324.51	328.68
C-C		59.712	57.892	59.140	59.698	59.494	58.920	58.585	58.865	59.536	59.528
	2	163.70	161.97	163.47	160.50	159.55	162.29	163.57	161.18	160.95	163.68
	3	320.15	319.68	314.86	313.16	320.00	314.61	313.20	320.15	314.56	318.76
	4	528.64	528.40	515.29	527.54	517.85	522.29	523.50	518.91	526.09	522.36
C-P	1	46.564	45.011	45.905	46.455	46.540	46.237	45.821	45.606	45.776	46.249
	2	138.41	136.57	138.39	136.47	134.83	136.17	138.28	137.51	135.49	136.37
	3	282.09	281.35	278.50	275.17	281.02	279.63	274.80	280.68	279.74	276.27
	4	477.71	477.68	465.89	475.08	471.19	468.12	476.84	466.07	477.69	467.55
S-S	1	25.207	25.172	25.061	24.892	24.710	24.571	24.528	24.611	24.815	25.068
	2	105.48	104.69	102.99	102.20	103.18	104.93	105.39	104.08	103.09	104.14
	3	236.35	232.53	229.20	233.38	236.20	231.44	231.18	236.17	233.34	231.71
	4	419.05	408.88	410.74	418.84	408.33	415.37	415.20	409.86	418.83	409.90

decreases as the mode order increases. Additionally, the natural frequencies are greatly affected under compressive loading rather than under tensile loading. The compressive loading leads to a decrease in the frequency, whereas tensile loading causes an increase of the frequency.

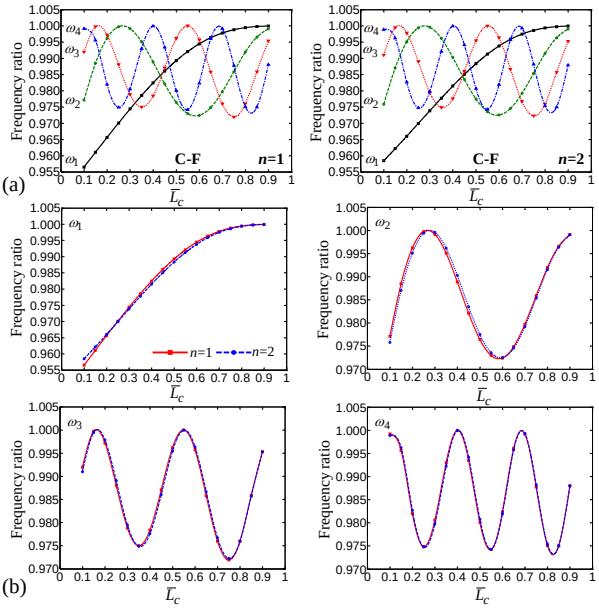

Fig. 7 Frequency ratio of the first four natural frequencies of tapered beams with a C-F end condition: (a) Effect of cracking on the first four modes for n=1 and n=2, (b) Comparison between n=1 and n=2 for each mode

The effect of axial loading on the first four mode shapes is illustrated in Fig. 5, which compares the results between n=1 and n=2. As expected, compressive loading attempts to bend the modes, with the reverse trend in effect for tensile loading.

Next, the effect of axial loading on the first four natural frequencies of single and double tapered beams with a C-F end condition is analyzed when the axial loading acts in an arbitrary distance x. The computed results are displayed in Table 4. Note that the application point of loading increases from a non-dimensional distance $\bar{L}(=x/L)$=0.1 to $\bar{L}$=1 in intervals of $\bar{L}$=0.1. Fig. 6(a) represents the effect of axial loading on the natural frequencies for single and double tapered beams, and Fig. 6(b) illustrates the comparison of the results computed from the two methods for each mode.

These effects are very small up to a non-dimensional distance of 0.2, but thereafter the natural frequencies vary greatly because of axial loading. In the above analysis, the effect of cracking on the natural frequencies of the tapered beams is ignored.

3.2 The effect of an open edge crack

The effect of cracking on the first four natural frequencies of single and double tapered beams is evaluated in the absence of axial loading. First, a single edge crack having s=0.5 is considered. The crack locations ($\bar{L}_c = L_c/L$) are assumed to vary from 0.1 to 0.9 in intervals of 0.1, and the taper ratio is 0.5. The eigenfrequencies of the tapered beams with an open edge crack are computed using four classical boundary conditions, that is, clamped-clamped (C-C), clamped-free (C-F), clamped-pinned (C-P), and simply supported (S-S) end conditions. The properties used are kept identical to those considered when the effect

Table 7 Effect of multiple edge cracks on the first four natural frequencies of a single tapered beam with different end conditions and taper ratios: n=1, F_0=0N

c	ω	Natural frequency (Hz)							
		C-F		C-C		C-P		S-S	
		Intact	Cracked	Intact	Cracked	Intact	Cracked	Intact	Cracked
0.0	1	12.742	12.584	81.029	80.763	55.848	55.000	35.745	35.196
	2	79.817	79.133	223.36	220.70	180.96	176.94	142.98	138.73
	3	223.46	218.77	437.88	426.38	377.56	367.54	321.70	312.25
	4	437.88	423.63	723.83	705.03	645.65	635.43	571.92	563.44
0.1	1	12.895	12.742	76.967	76.727	53.805	53.002	33.943	33.446
	2	77.319	76.672	212.16	209.75	172.61	169.09	135.82	132.04
	3	213.71	209.52	415.91	405.44	359.35	350.70	305.59	297.16
	4	417.38	404.56	687.51	671.17	613.98	605.42	543.25	536.11
0.2	1	13.075	12.922	72.754	72.515	51.662	50.895	32.054	31.600
	2	74.720	74.089	200.52	198.34	163.94	160.90	128.44	125.09
	3	203.61	199.88	393.09	383.66	340.44	333.12	288.90	281.43
	4	396.12	384.70	649.78	635.86	581.10	573.99	513.53	507.53
0.3	1	13.286	13.135	68.409	68.158	49.425	48.694	30.082	29.670
	2	72.037	71.421	188.52	186.54	154.99	152.40	120.85	117.93
	3	193.21	189.92	369.52	361.21	320.92	314.90	271.73	265.22
	4	374.19	364.19	610.80	599.34	547.14	541.36	482.89	477.95
0.4	1	13.541	13.390	63.902	63.627	47.071	46.380	28.008	27.637
	2	69.259	68.656	176.04	174.26	145.70	143.55	113.03	110.53
	3	182.46	179.58	345.03	337.92	300.66	295.90	253.97	248.42
	4	351.46	342.91	570.28	561.28	511.87	507.25	451.14	447.12
0.5	1	13.855	13.705	59.192	58.883	44.570	43.923	25.805	25.477
	2	66.373	65.783	162.99	161.41	135.98	134.24	104.91	102.83
	3	171.26	168.79	319.37	313.56	279.45	275.91	235.45	230.87
	4	327.75	320.67	527.82	521.19	474.95	471.24	417.98	414.72

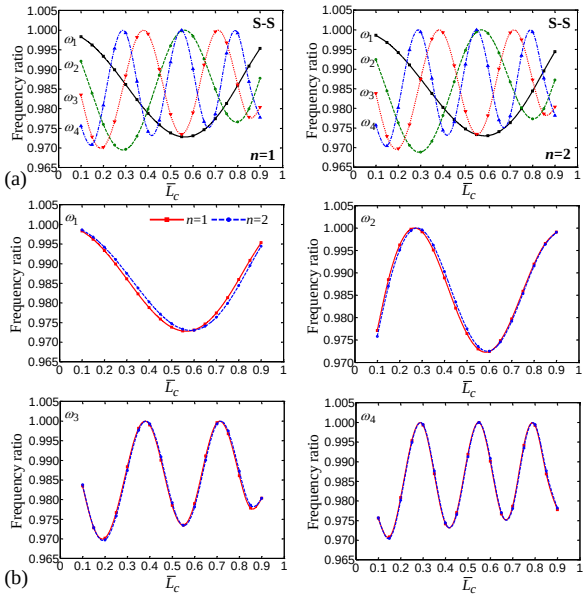

Fig. 8 Frequency ratio of the first four natural frequencies of tapered beams with an S-S end condition: (a) Effect of cracking on the first four modes for n=1 and n=2, (b) Comparison between n=1 and n=2 for each mode

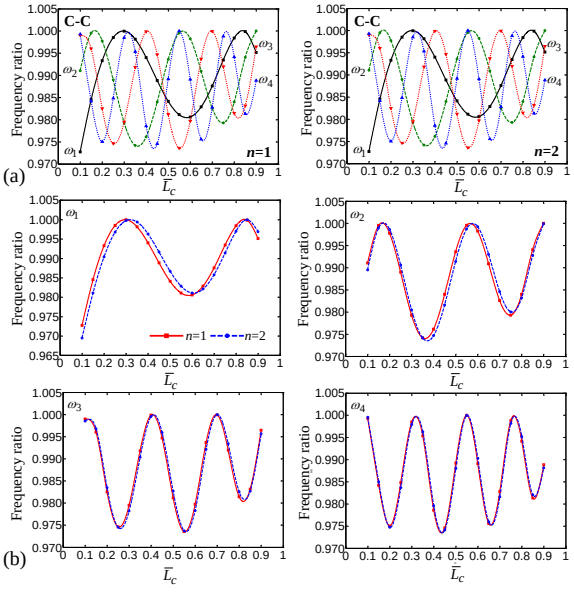

Fig. 9 Frequency ratio of the first four natural frequencies of tapered beams with a C-C end condition: (a) Effect of cracking on the first four modes for n=1 and n=2, (b) Comparison between n=1 and n=2 for each mode

Table 8 Effect of multiple edge cracks on the first four natural frequencies of a double tapered beam with different end conditions and taper ratios: n=2, F_0=0N

c	ω	Natural frequency (Hz)							
		C-F		C-C		C-P		S-S	
		Intact	Cracked	Intact	Cracked	Intact	Cracked	Intact	Cracked
0.0	1	12.746	12.586	81.029	80.767	55.852	55.005	35.745	35.197
	2	79.825	79.139	223.36	220.71	180.97	176.95	142.98	138.74
	3	223.47	218.78	437.88	426.40	377.56	367.56	321.70	312.26
	4	437.89	423.65	723.83	705.06	645.65	635.46	571.92	563.45
0.1	1	13.312	13.154	76.983	76.737	54.189	53.370	33.925	33.425
	2	78.087	77.427	212.18	209.77	172.99	169.49	135.84	132.07
	3	214.47	210.27	415.93	405.45	359.74	351.14	305.62	297.19
	4	418.15	405.31	687.54	671.25	614.37	605.83	543.28	536.16
0.2	1	13.969	13.806	72.820	72.563	52.434	51.634	31.976	31.516
	2	76.299	75.640	200.62	198.42	164.75	161.74	128.51	125.18
	3	205.20	201.46	393.19	383.77	341.27	334.04	289.02	281.57
	4	397.73	386.29	649.89	636.10	581.95	574.89	513.67	507.71
0.3	1	14.736	14.568	68.569	68.278	50.590	49.812	29.895	29.475
	2	74.483	73.823	188.73	186.74	156.27	153.73	121.03	118.13
	3	195.72	192.42	369.76	361.50	322.27	316.39	272.01	265.54
	4	376.76	366.74	611.05	599.81	548.52	542.80	483.22	478.32
0.4	1	15.649	15.474	64.208	63.867	48.641	47.890	27.652	27.274
	2	72.651	71.988	176.46	174.66	147.52	145.42	113.37	110.91
	3	186.01	183.12	345.48	338.51	302.60	298.03	254.50	249.01
	4	355.12	346.56	570.76	562.06	513.88	509.30	451.77	447.79
0.5	1	16.759	16.577	59.712	59.308	46.564	45.849	25.207	24.871
	2	70.831	70.164	163.70	162.09	138.41	136.74	105.48	103.45
	3	176.03	173.52	320.15	314.56	282.09	278.78	236.35	231.85
	4	332.68	325.61	528.64	522.35	477.71	474.01	419.05	415.79

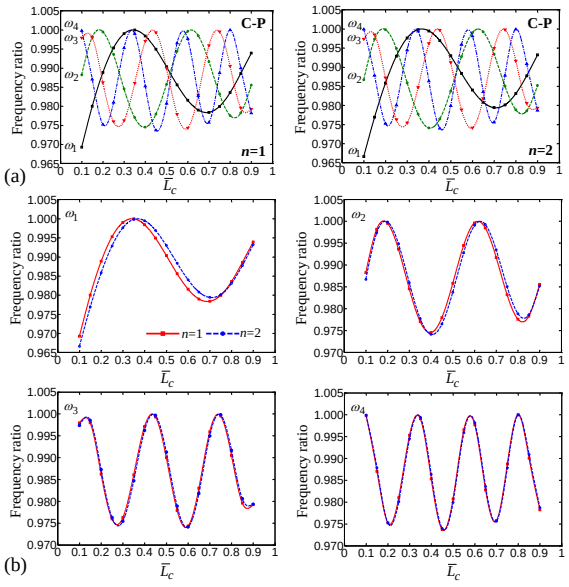

Fig. 10 Frequency ratio of the first four natural frequencies of tapered beams with a C-P end condition: (a) Effect of cracking on the first four modes for n=1 and n=2, (b) Comparison between n=1 and n=2 for each mode

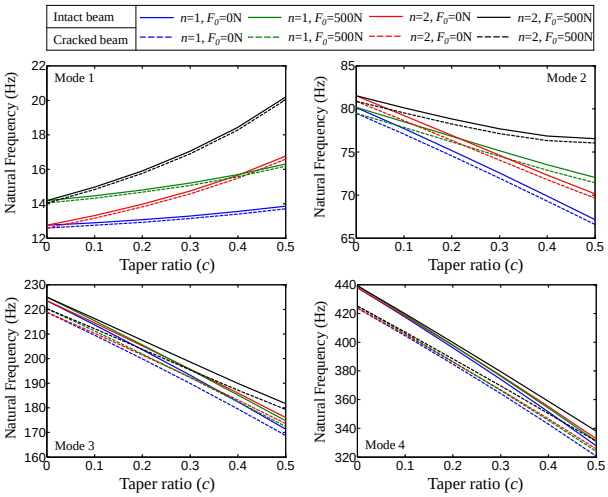

Fig. 11 Effect of multiple edge cracks and axial loading compared for each mode of single and double tapered beams with a C-F boundary condition

of axial loading was analyzed, and, unless otherwise mentioned, all examples will be evaluated by employing the

Table 9 Effect of multiple edge cracks and axial loading on the first four natural frequencies of a single tapered beam with C-F end conditions under different taper ratios

		Natural frequency (Hz)									
c	ω	F_0=100N		F_0=200N		F_0=300N		F_0=400N		F_0=500N	
		Intact	Cracked	Intact	Cracked	Intact	Cracked	Intact	Cracked	Intact	Cracked
0.0	1	13.044	12.890	13.337	13.188	13.622	13.476	13.900	13.757	14.171	14.031
	2	80.158	79.482	80.497	79.830	80.835	80.176	81.171	80.520	81.505	80.862
	3	223.75	219.07	224.04	219.37	224.33	219.67	224.62	219.97	224.91	220.27
	4	438.16	423.91	438.43	424.20	438.71	424.48	438.98	424.77	439.25	425.05
0.1	1	13.227	13.078	13.548	13.403	13.859	13.718	14.161	14.023	14.454	14.320
	2	77.706	77.069	78.090	77.463	78.473	77.855	78.853	78.244	79.231	78.632
	3	214.05	209.86	214.38	210.21	214.71	210.55	215.04	210.89	215.37	211.23
	4	417.69	404.88	418.01	405.21	418.32	405.53	418.63	405.85	418.94	406.18
0.2	1	13.442	13.295	13.797	13.654	14.140	14.000	14.471	14.334	14.791	14.658
	2	75.166	74.547	75.609	75.001	76.049	75.452	76.485	75.899	76.918	76.343
	3	204.00	200.28	204.39	200.68	204.77	201.07	205.15	201.47	205.54	201.87
	4	396.48	385.07	396.84	385.45	397.20	385.82	397.56	386.19	397.92	386.56
0.3	1	13.699	13.553	14.095	13.953	14.475	14.337	14.841	14.706	15.194	15.062
	2	72.561	71.958	73.079	72.489	73.592	73.016	74.101	73.538	74.605	74.055
	3	193.67	190.39	194.13	190.87	194.59	191.34	195.04	191.81	195.50	192.28
	4	374.62	364.63	375.05	365.07	375.48	365.51	375.90	365.95	376.33	366.39
0.4	1	14.012	13.866	14.459	14.318	14.886	14.748	15.294	15.160	15.686	15.554
	2	69.886	69.300	70.506	69.936	71.118	70.564	71.723	71.185	72.321	71.797
	3	183.02	180.16	183.57	180.74	184.13	181.31	184.68	181.88	185.24	182.45
	4	351.99	343.45	352.51	343.98	353.03	344.51	353.55	345.04	354.07	345.57
0.5	1	14.401	14.256	14.914	14.774	15.399	15.263	15.860	15.727	16.299	16.168
	2	67.148	66.579	67.910	67.362	68.659	68.130	69.396	68.886	70.121	69.628
	3	171.97	169.52	172.68	170.25	173.38	170.97	174.07	171.69	174.77	172.40
	4	328.41	321.34	329.08	322.01	329.74	322.68	330.40	323.35	331.05	324.01

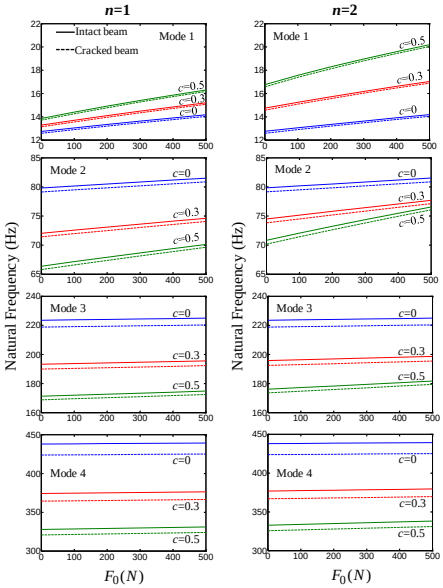

Fig. 12 Effect of tapering and cracking on the first four natural frequencies of tapered beams with a C-F end condition depending on the axial loading variation

Table 10 Effect of multiple edge cracks and axial loading on the first four natural frequencies of a double tapered beam with C-F end conditions under different taper ratios

		Natural frequency (Hz)									
c	ω	F_0=100N		F_0=200N		F_0=300N		F_0=400N		F_0=500N	
		Intact	Cracked	Intact	Cracked	Intact	Cracked	Intact	Cracked	Intact	Cracked
0.0	1	13.048	12.893	*13.342*	*13.191*	13.627	13.480	13.905	13.761	14.175	14.035
	2	80.166	79.489	*80.505*	*79.837*	80.843	80.183	81.179	80.527	81.514	80.870
	3	223.76	219.08	*224.05*	*219.38*	224.34	219.68	224.63	219.98	224.92	220.28
	4	438.17	423.94	*438.44*	*424.23*	438.72	424.51	438.99	424.80	439.26	425.08
0.1	1	13.664	13.510	*14.004*	*13.855*	14.333	14.187	14.652	14.510	14.962	14.823
	2	78.501	77.852	*78.912*	*78.273*	79.320	78.692	79.726	79.108	80.129	79.521
	3	214.83	210.64	*215.18*	*211.01*	215.54	211.38	215.89	211.75	216.24	212.11
	4	418.48	405.66	*418.81*	*406.00*	419.15	406.35	419.48	406.69	419.81	407.04
0.2	1	14.386	14.228	*14.786*	*14.633*	15.171	15.022	15.543	15.397	15.902	15.759
	2	76.813	76.168	*77.322*	*76.691*	77.827	77.210	78.328	77.724	78.825	78.233
	3	205.65	201.93	*206.10*	*202.39*	206.54	202.85	206.99	203.31	207.43	203.77
	4	398.15	386.72	*398.57*	*387.16*	398.98	387.59	399.40	388.02	399.82	388.45
0.3	1	15.240	15.077	*15.719*	*15.561*	16.177	16.023	16.615	16.465	17.035	16.888
	2	75.139	74.498	*75.788*	*75.165*	76.429	75.824	77.062	76.474	77.688	77.117
	3	196.31	193.03	*196.89*	*193.63*	197.47	194.23	198.05	194.83	198.62	195.42
	4	377.30	367.30	*377.85*	*367.86*	378.39	368.42	378.93	368.97	379.47	369.53
0.4	1	16.272	16.104	*16.857*	*16.695*	17.410	17.251	17.933	17.778	18.431	18.279
	2	73.521	72.884	*74.375*	*73.763*	75.215	74.627	76.040	75.474	76.851	76.307
	3	186.81	183.94	*187.60*	*184.76*	188.38	185.58	189.17	186.39	189.94	187.19
	4	355.87	347.32	*356.61*	*348.07*	357.35	348.83	358.09	349.58	358.83	350.33
0.5	1	17.554	17.380	*18.285*	*18.116*	18.963	18.798	19.595	19.434	20.189	20.030
	2	72.040	71.411	*73.215*	*72.621*	74.357	73.795	75.468	74.936	76.551	76.046
	3	177.18	174.71	*178.31*	*175.89*	179.44	177.05	180.55	178.21	181.66	179.35
	4	333.77	326.70	334.85	327.79	335.92	328.87	336.99	329.95	338.05	331.02

same properties. The first four eigenfrequencies for the in-plane bending vibrations of single (n=1) and double (n=2) tapered beams with a crack are tabulated in Tables 5 and 6. The results computed by applying n=1 are given in Table 5, and Table 6 reports the computed results for n=2.

These effects are illustrated in Figs. 7 and 10 as the frequency ratio with respect to variations of the crack location for each end condition. Based on the results in Tables 5 and 6, additional crack locations are considered. Figs. 7(a)-10(a) present the effect of cracking for n=1 and n=2, and Figs. 7(b)-10(b) represent each mode to compare the effects of the cracks between n=1 and n=2. The first and second natural frequencies for all boundary conditions show slight differences, but the third and fourth natural frequencies have similar effects. In particular, the effect of cracking is greater on the fundamental frequency when a C-F end condition is used. It is a well-known phenomenon that the fundamental frequency is sharply reduced when the crack location is closer to the fixed end. Further, the effects of cracking for the tapered beams are equal.

3.3 The effect of multiple open edge cracks and axial loading

Finally, the effect of multiple cracks and axial loading on the first four natural frequencies for the in-plane bending vibrations of single and double tapered beams is analyzed. The results provided in Tables 7 and 8 are obtained in the absence of axial loading. Three cracks with s=0.3, 0.2, and 0.4 are assumed to be located at the distance $\bar{L}_c$, where $\bar{L}_c$=0.2, 0.6, and 0.8 from point O, as shown in Figs. 1a and 1e. The results computed for the cracked and tapered beams with the four end conditions are compared between the intact and cracked beams, and a diverse set of taper ratios is examined.

Tables 9 and 10 present the results for the effects of both multiple cracks and tensile loadings. Tensile loading is assumed to act at the free end while taking into account the C-F end condition. Fig. 11 illustrates the mode variation for intact and cracked beams, considering the effect of both cracking and tensile loading as a function of an increase of the taper ratio. To illustrate, the results when F_0=0 and 500 N are analyzed. As shown for each mode between n=1 and n=2, the natural frequencies of tapered beams with cracks are reduced, having nearly similar trends compared with those of an intact beam regardless of the taper ratios. In particular, the first and second modes of the tapered beams are varied by consideration of the intact beam results. Fig. 12 presents the variation of the natural frequencies for single and double tapered beams with different taper ratios with respect to changing the tensile loading. All of the results increase linearly because of the tensile loading increase.

4. Conclusions

In this study, a transfer matrix method has been proposed to analyze the eigenpairs for two types of tapered beams with axial loading. Further, a straightforward method is proposed that is capable of evaluating effects of cracking on the natural frequencies for the bending vibrations of these beams. The accuracy of the presented method is demonstrated via comparison of the analyzed results, which show excellent agreement. The natural frequencies are greatly affected under compressive loading rather than under tensile loading. The compressive loading leads to a decrease in the frequency, whereas tensile loading causes an increase of the frequency. In addition, the eigenfrequencies on two types of tapered beams with cracks are reduced, having nearly similar trends compared with those of an intact beam regardless of the taper ratios.

Consequently, this work fully examines the effect of cracking and axial loading for two types of tapered beams. A comparison of the effects of axial loading and cracking on the natural frequencies of single and double tapered beams is expected to be useful in the design or assessment of beam-like tapered structures.

Acknowledgments

This work was supported by Kyonggi University Research Grant 2016.

References

Attar, M. (2012), "A transfer matrix method for free vibration analysis and crack identification of stepped beams with multiple edge cracks and different boundary conditions", *Int. J. Mech. Sci.*, **57**(1), 19-33.

Banerjee, J.R., Su, H. and Jackson, D.R. (2006), "Free vibration of rotating tapered beams using the dynamic stiffness method", *J. Sound Vibr.*, **298**(4-5), 1034-1054.

Behzad, M., Ghadami, A., Maghsoodi, A. and Hale, J.M. (2013), "Vibration based algorithm for crack detection in cantilever beam containing two different types of cracks", *J. Sound Vibr.*, **332**(24), 6312-6320.

Broda, D., Pieczonka, L., Hiwarkar, V., Staszewski, W.J. and Silberschmidt, V.V. (2016), "Generation of higher harmonics in longitudinal vibration of beams with breathing cracks", *J. Sound Vibr.*, **381**, 206-219.

Caddemi, S. and Morassi, A. (2013), "Multi-cracked euler-bernoulli beams: Mathematical modeling and exact solutions", *Int. J. Sol. Struct.*, **50**(6), 944-956.

Caddemi, S. and Calio, I. (2009), "Exact closed-form solution for the vibration modes of the euler-bernoulli beam with multiple open cracks", *J. Sound Vibr.*, **327**(3-5), 473-489.

Chaudhari, T.D. and Maiti, S.K. (1999), "Modelling of transverse vibration of beam of linearly variable depth with edge crack", *Eng. Fract. Mech.*, **63**(4), 425-445.

Cheng, Y., Yu, Z., Wu, X. and Yuan, Y. (2011), "Vibration analysis of a cracked rotating tapered beam using the p-version finite element method", *Finit. Elem. Anal. Des.*, **47**(7), 825-834.

Chondros, T.G., Dimarogonas, A.D. and Yao, J. (1998), "A continuous cracked beam vibration theory", *J. Sound Vibr.*, **215**(1), 17-34.

Dimogoronas, A.D. (1996), "Vibration of cracked structures: A state of the art review", *Eng. Fract. Mech.*, **55**(5), 831-857.

Donà, M., Palmeri, A. and Lombardo, M. (2015), "Dynamic analysis of multi-cracked euler-bernoulli beams with gradient elasticity", *Comput. Struct.*, **161**, 64-76.

Fernández-Sáez, J., Morassi, A., Pressacco, M. and Rubio, L. (2016), "Unique determination of a single crack in a uniform simply supported beam in bending vibration", *J. Sound Vibr.*, **371**, 94-109.

Hodges, D.H. and Rutkowski, M.J. (1981), "Free-vibration ananlysis of rotating beams by a variable-order finite element method", *AIAA J.*, **19**(11), 1459-1466.

Kisa, M. and Gurel, M.A. (2007), "Free vibration analysis uniform and stepped cracked beams with circular cross sections", *Int. J. Eng. Sci.*, **45**(2-8), 364-380.

Kundu, B. and Ganguli, R. (2017), "Analysis of weak solution of euler-bernoulli beam with axial force", *Appl. Math. Comput.*, **298**, 247-260.

Lee, J.H. (2009), "Identification of multiple cracks in a beam using vibration amplitudes", *J. Sound Vibr.*, **326**(1-2), 205-212.

Lee, J.W. and Lee, J.Y. (2016), "Free vibration analysis using the transfer-matrix method on a tapered beam", *Comput. Struct.*, **164**, 75-82.

Lee, J.W. and Lee, J.Y. (2017a), "A transfer matrix method capable of determining the exact solutions of a twisted bernoulli-euler beam with multiple edge cracks", *Appl. Math. Model.*, **41**, 474-493.

Lee, J.W. and Lee, J.Y. (2017b), "In-plane bending vibration analysis of a rotating beam with multiple edge cracks by using the transfer matrix method", *Mecc.*, **52**(4-5), 1143-1157.

Lee, Y.S. and Chung, M.J. (2000), "A study on crack detection using eigenfrequency test data", *Comput. Struct.*, **77**(3), 327-

342.
Li, X.F., Tang, A.Y. and Xi, L.Y. (2013), "Vibration of a rayleigh cantilever beam with axial force and tip mass", *J. Constr. Steel. Res.*, **80**, 15-22.
Loya, J.A., Rubio, L. and Fernández-Sáez, J. (2006), "Natural frequencies for bending vibrations of Timoshenko cracked beams", *J. Sound Vibr.*, **290**(3-5), 640-653.
Mazanoglu, K. and Sabuncu, M. (2010), "Vibration analysis of non-uniform beams having multiple edge cracks along the beam's height", *Int. J. Mech. Sci.*, **52**(3), 515-522.
Nahvi, H. and Jabbari, M. (2005), "Crack detection in beams using experimental modal data and finite element model", *Int. J. Mech. Sci.*, **47**(10), 1477-1497.
Neves, A.C., Simões, F.M.F. and Pinto Da Costa, A. (2016), "Vibrations of cracked beams: Discrete mass and stiffness models", *Comput. Struct.*, **168**, 68-77.
Rossit, C.A., Bambill D.V. and Gilardi G.J. (2017), "Free vibrations of AFG cantilever tapered beams carrying attached masses", *Struct. Eng. Mech.*, **61**(5), 685-691.
Ruotolo, R. and Surace, C. (1997), "Damage assessment of multiple cracked beams: Numerical results and experimental validation", *J. Sound Vibr.*, **206**(4), 567-588.
Sarkar, K., Ganguli, R. and Elishakoff, I. (2016), "Closed-form solutions for non-uniform axially loaded rayleigh cantilever beams", *Struct. Eng. Mech.*, **60**(3), 455-470.
Sarkar, K. and Ganguli, R. (2014), "Modal tailoring and closed-form solutions for rotating non-uniform euler-bernoulli beams", *Int. J. Mech. Sci.*, **88**, 208-220.
Skrinar, M. (2009), "Elastic beam finite element with an arbitrary number of transverse cracks", *Finit. Elem. Anal. Des.*, **45**(3), 181-189.
Sun, W., Sun, Y., Yu, Y. and Zheng, S. (2016), "Nonlinear vibration analysis of a type of tapered cantilever beams by using an analytical approximate method", *Struct. Eng. Mech.*, **59**(1), 1-14.
Vinod, K.G., Gopalakrishnan, S. and Ganguli, R. (2007), "Free vibration and wave propagation analysis of uniform and tapered rotating beams using spectrally formulated finite elements", *Int. J. Sol. Struct.*, **44**(18-19), 5875-5893.
Wauer, J. (1990), "On the dynamics of cracked rotors: A literature survey", *Appl. Mech. Rev.*, **43**(1), 13-17.
Yan, Y., Ren, Q., Xia, N. and Zhang, L. (2016), "A closed-form solution applied to the free vibration of the euler-bernoulli beam with edge cracks", *Arch. Appl. Mech.*, **86**(9), 1633-1646.
Yuan, J.H., Pao, Y.H. and Chen, W.Q. (2016), "Exact solutions for free vibrations of axially inhomogeneous Timoshenko beams with variable cross section", *Mecc.*, **227**(9), 2625-2643.
Zhang, K. and Yan, X. (2016), "Multi-cracks identification method for cantilever beam structure with variable cross-sections based on measured natural frequency changes", *J. Sound Vibr.*, **387**, 53-65.
Zhou, Y., Zhang, Y. and Yao, G. (2017), "Stochastic forced vibration analysis of a tapered beam with performance deterioration", *Acta Mech.*, **228**(4), 1393-1406.